International Journal of Control
Vol. 00, No. 00, Month 200x, 1–25

Analytical and Graphical Design of Lead-Lag Compensators

Roberto & Zanasi[a]*, Stefania & Cuoghi[a] and Lorenzo & Ntogramatzidis[b].

[a] *DII-Information Engineering Department, University of Modena and Reggio Emilia, Modena, Italy.*
[b]*Department of Mathematics and Statistics, Curtin University, Perth, Australia.*

(*vx.x released August 2011*)

In this paper an approach based on inversion formulae is used for the design of lead-lag compensators which satisfy frequency domain specifications on phase margin, gain margin and phase (or gain) crossover frequency. An analytical and graphical procedure for the compensator design on the Nyquist and Nichols planes is presented with some numerical examples.

Keywords: linear control; robust control; Nyquist diagram; Nichols diagram

1 Introduction

Lead, lag and lead-lag compensators are among the most utilised control architectures in industrial and process engineering, and for this reason they have always received a great deal of attention ‘(Franklin, Powell and Emami-Naeini 2006)’. The recent literature shows a renewed interest in the design of lead/lag-type controllers ‘(Messner, Bedillion, Xia and Karns 2007, Messner 2009)’ for classical loop shaping and weighting functions for automated controller synthesis algorithms ‘(Messner 2009)’. Lead and lag compensators are characterised by a simple first-order model and, in addition to their DC gain which is usually selected on the basis of the steady-state performance specifications, they are described by two parameters, which are the time constants of the real zero and of the real pole. The lead-lag compensator has a richer dynamic structure, since it is characterised by a second-order transfer function with two poles and two zeros. The additional parameter of lead-lag compensators enables extra specifications to be imposed, to the expense of the increased complexity. In this paper we focus our attention on the classic frequency domain specifications, i.e., specifications on the phase and gain margins (GPM) and on the gain and phase crossover frequencies.

Specifications on the phase and gain margins have always been extensively utilised in feedback control system design to ensure a desirable performance and to obtain a robust control system. Moreover, specifications on phase margin and gain crossover frequency are common because these two parameters together often serve as a measure of the performance of a control system. Indeed, the phase margin is loosely related to characteristics of the response such as the peak overshoot and the resonant peak, while the gain crossover frequency is known to affect the rise time and the bandwidth, ‘(Franklin et al. 2006)’.

The classical tuning methods for lead, lag and lead-lag compensators employing Bode and Nichols diagrams are based on trial-and-error and/or heuristic techniques, and are therefore approximate by nature. The main drawback of the trial-and-error method, which is usually based on considerations on the Bode plot, is that this method often leads to a controller that does not behave as expected. For example, in the case one wants to obtain a certain phase lead in the loop gain transfer function, the main idea is to place the frequency where the compensator attains the maximum phase lead at a frequency that

*Corresponding author. Email: roberto.zanasi@unimore.it

ISSN: 0020-7179 print/ISSN 1366-5820 online

DOI: 10.1080/0020717YYxxxxxxxx
http://www.informaworld.com

is slightly greater than the gain crossover frequency of the plant, because a lead compensator amplifies the magnitude of the plant over the entire spectrum; this frequency is usually selected by rule of thumb. However, since in this way we cannot predict what the new crossover frequency of the loop gain will be, it is far from certain that the loop gain transfer function will have an improvement in the phase margin with respect to the uncompensated system. A similar problem occurs for lag and lead-lag compensators. Another consequence of the clumsiness associated with the classic trial-and-error design method is the fact that this procedure is difficult to automate into an algorithm, and is therefore unsuited to be used as a self-tuning strategy.

However, in recent times different methods have been proposed for the computation of the parameters of the controller to satisfy GPM specifications, for lead, lag, lead-lag compensators as well as for compensators in the family of PID controllers to the end of avoiding the trial-and-error nature of classical control methods, '(Åström and Hagglund 1984, Ho, Gan, Tay and Ang 1996, Fung, Wang and Lee 1998, Wang, Fung and Zhang 1999, Lee 2004, Flores, Valle and Castillejos 2007)'.

The approach proposed in '(Yeung, Wong and Chen 1998)' is based on a graphical construction on Bode and Nichols plots, and can handle specifications on the steady-state performance, gain and phase margins and gain or phase crossover frequency.

A control technique recently introduced for the computation of the parameters of the compensator is based on a closed-form formula that expresses the frequency response of the compensator at a generic frequency in polar form. Since the GPM and crossover frequency specifications result in the assignment of the magnitude and argument of the frequency response of the compensator at the desired gain or phase crossover frequency, these formulae enable the parameters of the compensators to be computed directly given the frequency domain specifications. These formulae first appeared for generic first-order compensators in '(Phillips 1985)', and their use and geometric interpretation in the context of control feedback design was detailed in '(Marro and Zanasi 1998)'. In the same spirit, a solution of a control problem with GPM and crossover frequency specifications has recently been proposed for PID controllers in '(Ntogramatzidis and Ferrante 2011)'.

Since the approach based on these inversion formulae is exact, in the case of first-order lead and lag networks – which we recall are characterised by two free parameters if one excludes the DC gain – only specifications on either the phase margin and the gain crossover frequency or on the gain margin and on the phase crossover frequency are allowed. Within the context of exact design with frequency domain specifications, the use of lead-lag compensators – also known as *notch compensators* – is particularly important. Indeed, on the one hand, when the phase margin and gain crossover frequency are imposed, the lead-lag network can be employed whenever a lead or a lag compensator can solve the problem, but there are cases in which a lead-lag compensator can satisfy the control specifications whereas a simple lead or lag network cannot (precisely, when the frequency response of the plant at the desired gain crossover frequency is such that its magnitude is greater than 1 and the difference between its argument and the desired phase margin is an angle greater than $\pi/2$ and smaller than π); similar considerations hold with requirements on the gain margin and phase crossover frequency. On the other hand, the degree of freedom of the extra parameter in the transfer function of the second-order lead-lag compensator can be exploited to satisfy an additional requirement/specification on the other margin. Notwithstanding the wealth of results in the area of tuning techniques of standard compensators, to the best of the authors' knowledge an exact method has never been proposed for the computation of the parameters of lead-lag networks in case of standard GPM and crossover frequencies specifications.

The method proposed in this paper is both analytic and graphical, in the sense that it can be carried out both by determining directly the parameters of the compensator as a function of the specifications and by making use of the Nyquist or Nichols plots. In this way, the advantages of analytic and graphic procedures are combined together to deliver a method that outperforms the classic techniques based on trial-and-error considerations. Differently from the method in '(Yeung et al. 1998)', in which the parameters of the compensator are determined using a graphic construction on a special design chart, the approach presented in this paper enables the parameters of the compensator to be computed *exactly* using simple formulae that are similar in spirit to those given in '(Phillips 1985)' and '(Marro and Zanasi 1998)', thus eliminating a major source of approximation. Moreover, the method proposed in this paper

enables *all* the solutions of the control problem to be computed, whereas all other graphical approaches such as '(Yeung et al. 1998)' can only deliver a subset of such solutions. This is a fundamental difference, because some of the solutions determined in '(Yeung et al. 1998)' can lead to negative (and therefore infeasible) values of the compensator parameters. Lastly, in the case of a lead-lag compensator there is a further educational advantage in the employment of Nyquist plots instead of Nichols or other types of charts, due to the fact that the polar plot of a lead-lag compensator is a simple circle. Therefore, the design can be successfully carried out using a compass and a ruler.

The paper is organized as follows. In Section II, we briefly recall the fundamental characteristics of lead-lag compensators, and the method based on inversion formulae is presented. In Section III a graphical interpretation of this method is given on the Nyquist plane. In Section IV, we introduce the five control problems studied in this paper, in which the parameters of a lead-lag compensator are sought to satisfy specifications on the GPM and on the crossover frequencies. Numerical examples and conclusions end the paper.

2 Lead-lag compensators: the general structure

Consider a lead-lag compensator described by the transfer function

$$C(s) = \frac{s^2 + 2\,\gamma\delta\,\omega_n\,s + \omega_n^2}{s^2 + 2\,\delta\,\omega_n\,s + \omega_n^2}, \tag{1}$$

where γ, δ and ω_n are real and positive. When $\gamma\delta < 1$ and/or $\delta < 1$ the zeros and/or the poles of the lead-lag compensator $C(s)$ are complex conjugate with negative real part. The compensator $C(s)$ has a unity static gain $C(0) = 1$ which does not change the static behavior (i.e., the steady-state performance) of the controlled system. The frequency response $C(j\omega)$ of the compensator $C(s)$ is

$$C(j\omega) = \frac{\omega_n^2 - \omega^2 + j\,2\,\gamma\delta\,\omega_n\omega}{\omega_n^2 - \omega^2 + j\,2\delta\,\omega_n\,\omega}, \tag{2}$$

which, for $\omega \neq \omega_n$, can be written as

$$C(j\omega) = \frac{1 + jX(\omega)}{1 + jY(\omega)} \tag{3}$$

where

$$X(\omega) = \frac{2\gamma\delta\,\omega\,\omega_n}{\omega_n^2 - \omega^2}, \qquad Y(\omega) = \frac{2\delta\,\omega\,\omega_n}{\omega_n^2 - \omega^2}. \tag{4}$$

Due to assumptions that γ, δ and ω_n are real and positive, functions $X(\omega)$ and $Y(\omega)$ satisfy

$$\begin{cases} X(\omega) > 0,\ Y(\omega) > 0 \text{ when } \ \omega < \omega_n, \\ X(\omega) < 0,\ Y(\omega) < 0 \text{ when } \ \omega > \omega_n. \end{cases} \tag{5}$$

The parameter γ is the gain of $C(j\omega)$ at frequency $\omega = \omega_n$. From (2) and (3) we get:

$$\gamma = C(j\omega_n) = \frac{X(\omega)}{Y(\omega)}\Big|_{\omega\neq\omega_n}. \tag{6}$$

The gain γ is the minimum (or maximum) amplitude of $C(j\omega)$. The Nyquist and Bode diagrams of

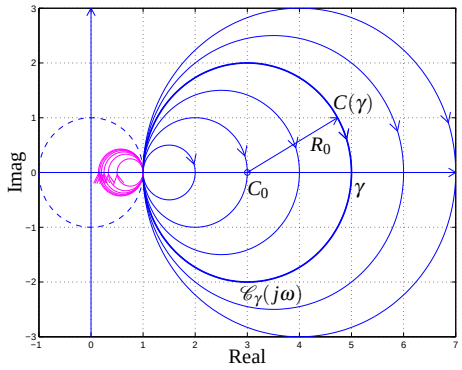

Figure 1. Nyquist diagrams of function $C(j\omega)$ when $\omega_n = 1$, ($\delta = 1.5$, $\gamma = [2:1:7]$, blue lines) and ($\delta = 1.5$, $\gamma = 1./[2:1:7]$, magenta lines). The thick blue line is for $\delta = 1.5$ and $\gamma = 5$.

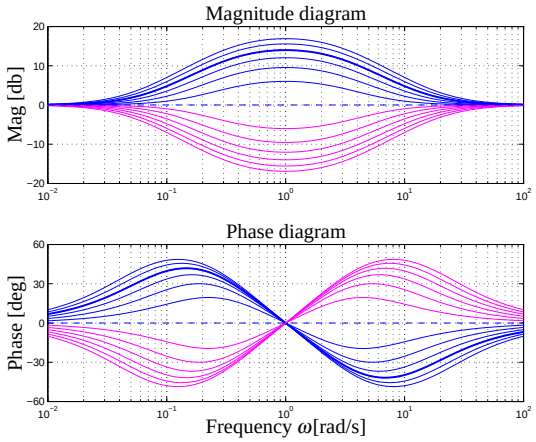

Figure 2. Bode diagrams of function $C(j\omega)$ when $\omega_n = 1$, ($\delta = 1.5$, $\gamma = [2:1:7]$, blue lines) and ($\delta = 1.5$, $\gamma = 1./[2:1:7]$, magenta lines). The thick blue line is for $\delta = 1.5$ and $\gamma = 5$.

$C(j\omega)$ for $\omega_n = 1$ and for different values of the parameters δ and γ are shown in Fig. 1 and Fig. 2. The Nyquist diagrams of Fig. 1 satisfy a property which is based in the following definition.

Definition 2.1: Let $\mathscr{C}(\gamma)$ denote the set of all the lead-lag compensators $C(s)$ as defined in (1) characterized by the same parameter γ, that is

$$\mathscr{C}(\gamma) = \left\{ C(s) \text{ as in (1)} \;\middle|\; \delta > 0, \omega_n > 0 \right\}. \tag{7}$$

Moreover, let $\mathscr{C}_\gamma(s) \in \mathscr{C}(\gamma)$ denote one element of $\mathscr{C}(\gamma)$ chosen arbitrarily.

Property 2.2 The shape of the frequency response $\mathscr{C}_\gamma(j\omega)$ of $\mathscr{C}_\gamma(s)$ on the Nyquist plane is a circle with center C_0 and radius R_0

$$C(\gamma) = C_0 + R_0 e^{j\theta}, \quad C_0 = \frac{\gamma+1}{2}, \quad R_0 = \frac{|\gamma-1|}{2} \tag{8}$$

where $\theta \in [0, 2\pi]$, see Fig. 1. The intersections of $\mathscr{C}_\gamma(j\omega)$ with the real axis occur at points 1 and γ. The shape does not depend on $\delta > 0$ and $\omega_n > 0$.

Proof: One can easily verify that the distance $d = |\mathscr{C}_\gamma(j\omega) - C_0|$ of the generic point $\mathscr{C}_\gamma(j\omega)$ from the

center C_0 is constant and equal to R_0:

$$\begin{aligned} d^2 = |\mathscr{C}_\gamma(j\omega) - C_0|^2 &= \left| \frac{\omega_n^2-\omega^2+j2\gamma\delta\omega_n\omega}{\omega_n^2-\omega^2+j2\delta\omega_n\omega} - \frac{\gamma+1}{2} \right|^2 \\ &= \left| \frac{2(\omega_n^2-\omega^2+j2\gamma\delta\omega_n\omega)-(\gamma+1)(\omega_n^2-\omega^2+j2\delta\omega_n\omega)}{2(\omega_n^2-\omega^2+j2\delta\omega_n\omega)} \right|^2 \\ &= \left| \frac{(1-\gamma)[(\omega_n^2-\omega^2)-j2\gamma\delta\omega_n\omega)]}{2(\omega_n^2-\omega^2+j2\delta\omega_n\omega)} \right|^2 = \left| \frac{\gamma-1}{2} \right|^2 = R_0^2. \end{aligned}$$

Variations of ω_n and δ modify the distribution of the frequency ω on the Nyquist diagram of $\mathscr{C}_\gamma(j\omega)$, but they do not change the diagram shape, which only depends on γ. ■

Remark 1: The considered lead-lag compensator $C(s)$ in (1) is a general form which encompasses the classical form $C_r(s)$ with real poles and real zeros

$$C_r(s) = \frac{(1+\tau_1 s)(1+\tau_2 s)}{(1+\alpha\tau_1 s)(1+\frac{\tau_2}{\alpha}s)} \tag{9}$$

with $0 < \tau_1 < \tau_2$ and $0 < \alpha < 1$. Details on the relations that link the parameters of the general and the classical forms $C(s)$ and $C_r(s)$ are given in Appendix A.

3 The controllable domain of lead-lag compensator $C(s)$

The concept of controllable domain introduced in this section is useful in the design of the lead-lag compensator $C(s)$.

Definition 3.1: **($\mathscr{D}^-$).** Let us define the "*controllable domain of a lead-lag compensator* $C(s)$" as

$$\mathscr{D}^- = \{z \in \mathbb{C} \,|\, \exists\, \gamma, \delta, \omega_n > 0, \exists\, \omega \geq 0 : \; C(j\omega)\cdot z = 1\}.$$

Loosely speaking, the *controllable domain* $\mathscr{D}^-$ can be interpreted as the set of all the points $z \in \mathbb{C}$ that "can be moved" to point 1 on the Nyquist plane by pre-multiplication with the frequency response $C(j\omega)$, where $C(s)$ is as in (1), for some $\omega \geq 0$ and for suitable values of the parameters $\gamma, \delta, \omega_n > 0$, see Fig. 3. It can be easily verified that domain $\mathscr{D}^-$ is given by $\mathscr{D}^- = \mathscr{D}_1^- \cup \mathscr{D}_2^-$ where

$$\mathscr{D}_1^- = \left\{ z = M e^{j\varphi} \;\middle|\; -\frac{\pi}{2} < \varphi < \frac{\pi}{2},\, M > \frac{1}{\cos\varphi} \right\},$$

$$\mathscr{D}_2^- = \left\{ z = M e^{j\varphi} \;\middle|\; -\frac{\pi}{2} < \varphi < \frac{\pi}{2},\, 0 < M < \cos\varphi \right\}.$$

Domain $\mathscr{D}_1^-$ is obtained when $\gamma > 1$ and domain $\mathscr{D}_2^-$ is obtained when $0 < \gamma < 1$. The shape of $\mathscr{D}^- = \mathscr{D}_1^- \cup \mathscr{D}_2^-$ on the Nyquist plane is shown in Fig. 3, see '(Marro and Zanasi 1998)'.

Definition 3.2: Let $\mathscr{C}^-(\gamma)$ denote the set of lead-lag compensators defined as

$$\mathscr{C}^-(\gamma) = \left\{ \frac{1}{C(s)} \;\middle|\; C(s) \in \mathscr{C}(\gamma) \right\}, \tag{10}$$

with $\mathscr{C}(\gamma)$ defined in (7). Moreover, let $\mathscr{C}_\gamma^-(s) \in \mathscr{C}^-(\gamma)$ denote one element of the set $\mathscr{C}^-(\gamma)$ chosen arbitrarily.

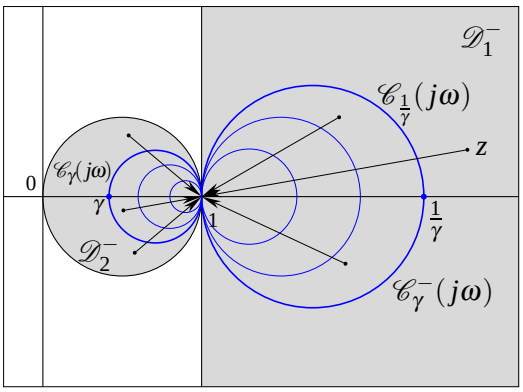

Figure 3. Controllable domain $\mathscr{D}^-$ of lead-lag compensators $C(s)$ on the Nyquist plane.

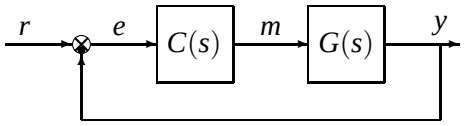

Figure 4. Unity feedback control structure.

Property 3.3 Given $\gamma > 0$, the two sets $\mathscr{C}^-(\gamma)$ and $\mathscr{C}(\frac{1}{\gamma})$ coincide, i.e.,

$$\mathscr{C}^-(\gamma) = \mathscr{C}(\tfrac{1}{\gamma}) \tag{11}$$

and the frequency responses $\mathscr{C}_\gamma^-(j\omega)$ and $\mathscr{C}_{\frac{1}{\gamma}}(j\omega)$ of $\mathscr{C}_\gamma^-(s)$ and $\mathscr{C}_{\frac{1}{\gamma}}(s)$ on the Nyquist plane have the same shape, see Fig. 3. The property holds also on the Nichols plane.

Proof: Each element $\mathscr{C}_\gamma^-(s)$ of $\mathscr{C}^-(\gamma)$ also belongs to $\mathscr{C}(\frac{1}{\gamma})$. In fact, from (7) and (10), it follows that

$$\mathscr{C}_\gamma^-(s) = \frac{s^2 + 2\delta\omega_n s + \omega_n^2}{s^2 + 2\gamma\delta\omega_n s + \omega_n^2} = \frac{s^2 + 2(\frac{1}{\gamma})\overline{\delta}\omega_n s + \omega_n^2}{s^2 + 2\overline{\delta}\omega_n s + \omega_n^2} \in \mathscr{C}(\tfrac{1}{\gamma}),$$

where $\overline{\delta} = \gamma\delta$. In the same way it can be easily proved that each element $\mathscr{C}_{\frac{1}{\gamma}}(s)$ of $\mathscr{C}(\frac{1}{\gamma})$ also belongs to $\mathscr{C}^-(\gamma)$, and therefore $\mathscr{C}^-(\gamma)$ and $\mathscr{C}(\frac{1}{\gamma})$ coincide. Moreover, the shape of the Nyquist diagrams of $\mathscr{C}_\gamma^-(s)$ and $\mathscr{C}_{\frac{1}{\gamma}}(s)$ depend only on γ and therefore they coincide. The extension of this property to Nichols diagrams is straightforward. ■

From (8) and (11) it follows that the Nyquist diagram of $\mathscr{C}_\gamma^-(s)$ is a circle whose center $C_0 = (\gamma+1)/(2\gamma)$ lies on the real axis, whose radius is $R_0 = |\gamma-1|/(2\gamma)$ and its intersections with the real axis occur at points $a = 1$ and $b = \frac{1}{\gamma}$, see Fig. 3.

4 Lead-lag compensators $C(s,\omega_n)$ moving a point A to a point B

Consider the block-diagram shown in Fig. 4, where $G(s)$ denotes the transfer function of the linear time-invariant plant to be controlled, which may have a transient delay and may include the gain and the integration terms required to meet the steady-state accuracy specifications. The lead-lag compensator $C(s)$ has to be designed in order to satisfy phase margin ϕ_m, gain margin G_m and gain (or phase) crossover frequency specifications.

Let $C(j\omega_0) = M_0 e^{j\varphi_0}$ denote the value of the frequency response $C(j\omega) = M(\omega)e^{j\varphi(\omega)}$ of the compensator $C(s)$ at frequency ω_0, where $M_0 = M(\omega_0)$ and $\varphi_0 = \varphi(\omega_0)$. To study how $C(j\omega)$ affects $G(j\omega)$ at frequency ω_0, let us consider two generic points $A = M_A e^{j\varphi_A}$ and $B = M_B e^{j\varphi_B}$ of the complex plane.

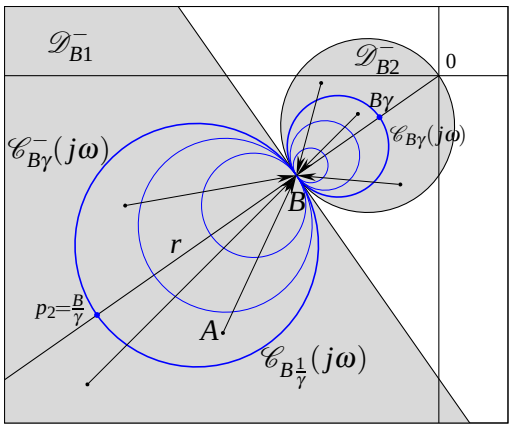

Figure 5. Controllable domain $\mathscr{D}_B^- = \mathscr{D}_{B1}^- \cup \mathscr{D}_{B2}^-$ on the Nyquist plane.

Referring to Fig. 5, we say that *point A is controllable to point B* (or equivalently that *point A can be moved to point B*) if a value $C(j\omega_0)$ exists such that

$$B = C(j\omega_0)\cdot A, \tag{12}$$

that is if and only if the following conditions hold:

$$M_B = M_A M_0, \qquad \varphi_B = \varphi_A + \varphi_0. \tag{13}$$

Definition 4.1: **($\mathscr{D}_B^-$).** Given a point $B \in \mathbb{C}$, let us define the "*controllable domain of the lead-lag compensator* $C(s)$ *to point B*" as

$$\mathscr{D}_B^- = \{A \in \mathbb{C} \,|\, \exists\, \gamma, \delta, \omega_n > 0, \exists\, \omega \geq 0 : \; C(j\omega)\cdot A = B\}.$$

Domain $\mathscr{D}_B^-$ is the set of all the points A of the complex plane that can be moved to point B using the compensator $C(s)$. One can easily verify that $\mathscr{D}_B^-$ can be expressed as $\mathscr{D}_B^- = \mathscr{D}_{B1}^- \cup \mathscr{D}_{B2}^-$ where

$$\mathscr{D}_{B1}^- = \left\{ A = M_A e^{j\varphi_A} \;\middle|\; -\frac{\pi}{2} + \varphi_B < \varphi_A < \frac{\pi}{2} + \varphi_B, \;\; M_A > \frac{M_B}{\cos(\varphi_A - \varphi_B)} \right\},$$

and

$$\mathscr{D}_{B2}^- = \left\{ A = M_A e^{j\varphi_A} \;\middle|\; -\tfrac{\pi}{2} + \varphi_B < \varphi_A < \tfrac{\pi}{2} + \varphi_B, \;\; 0 < M_A < M_B \cos(\varphi_A - \varphi_B) \right\},$$

see Fig. 5.

Definition 4.2: Given $B \in \mathbb{C}$, let $\mathscr{C}_B(\gamma)$ and $\mathscr{C}_B^-(\gamma)$ denote the sets of lead-lag compensators $C(s)$ defined as

$$\mathscr{C}_B(\gamma) = \left\{ B\cdot C(s) \,|\, C(s) \in \mathscr{C}(\gamma) \right\} \tag{14}$$

$$\mathscr{C}_B^-(\gamma) = \left\{ \frac{B}{C(s)} \;\middle|\; C(s) \in \mathscr{C}(\gamma) \right\} \tag{15}$$

with $\mathscr{C}(\gamma)$ defined in (7). Moreover, let $\mathscr{C}_{B\gamma}(s) \in \mathscr{C}_B(\gamma)$ and $\mathscr{C}^-_{B\gamma}(s) \in \mathscr{C}^-_B(\gamma)$ denote particular elements of the two sets $\mathscr{C}_B(\gamma)$ and $\mathscr{C}^-_B(\gamma)$ chosen arbitrarily.

Property 4.3 Given $\gamma > 0$, the two sets $\mathscr{C}^-_B(\gamma)$ and $\mathscr{C}_B(\frac{1}{\gamma})$ coincide, i.e.,

$$\mathscr{C}^-_B(\gamma) = \mathscr{C}_B(\tfrac{1}{\gamma}), \tag{16}$$

and the Nyquist diagram of the frequency responses $\mathscr{C}^-_{B\gamma}(j\omega)$ and $\mathscr{C}_{B\frac{1}{\gamma}}(j\omega)$ of $\mathscr{C}^-_{B\gamma}(s)$ and $\mathscr{C}_{B\frac{1}{\gamma}}(s)$ have the same shape. The intersections p_1 and p_2 of $\mathscr{C}^-_{B\gamma}(j\omega)$ with the straight line r passing through points 0 and B are $p_1 = B$ and $p_2 = \frac{B}{\gamma}$. The corresponding graphical representation is shown in Fig. 5.

Proof: Property 4.3 follows directly from Property 3.3 because $\mathscr{C}^-_B(\gamma) = B \cdot \mathscr{C}^-(\gamma) = B \cdot \mathscr{C}(\frac{1}{\gamma})$. ■

Definition 4.4: ***(Inversion Formulae).*** Given two points $A = M_A e^{j\varphi_A}$ and $B = M_B e^{j\varphi_B}$ of the complex plane $\mathbb{C}$, the inversion formulae $X(A,B)$ and $Y(A,B)$ are defined as follows

$$\begin{aligned} X(A,B) &= \frac{M - \cos\varphi}{\sin\varphi}, \\ Y(A,B) &= \frac{\cos\varphi - \dfrac{1}{M}}{\sin\varphi}, \end{aligned} \tag{17}$$

where

$$M = \frac{M_B}{M_A}, \qquad \varphi = \varphi_B - \varphi_A. \tag{18}$$

These formulae are similar to the ones used in '(Phillips 1985)' and are the same *inversion formulae* introduced and used in '(Marro and Zanasi 1998)' and '(Zanasi and Morselli 2009)' for the continuous-time case. The following property shows how the *inversion formulae* can be efficiently employed in the design of a lead-lag compensators $C(s)$.

Property 4.5 ***(From A to B).*** Given a point $B \in \mathbb{C}$ and chosen a point A of the frequency response $G(j\omega)$ at frequency ω_A belonging to the controllable domain $\mathscr{D}^-_B$, i.e. $A = G(j\omega_A) \in \mathscr{D}^-_B$, the set $C(s,\omega_n)$ of all the lead-lag compensators $C(s)$ that move point A to point B is obtained from (1) using

$$\gamma = \frac{X}{Y} > 0, \qquad \delta = Y\frac{\omega_n^2 - \omega_A^2}{2\omega_n\omega_A} > 0, \tag{19}$$

for all $\omega_n > 0$ such that $\delta > 0$ and with $X = X(A,B)$ and $Y = Y(A,B)$ obtained using (17).

Proof: For $\omega = \omega_A$, (4) can be rewritten as

$$\gamma = \frac{X(\omega_A)}{Y(\omega_A)}, \qquad \delta = Y(\omega_A)\frac{\omega_n^2 - \omega_A^2}{2\omega_n\omega_A}.$$

Substituting in (1) one obtains

$$C(s,\omega_n) = \frac{s^2 + X\frac{\omega_n^2 - \omega_A^2}{\omega_A}s + \omega_n^2}{s^2 + Y\frac{\omega_n^2 - \omega_A^2}{\omega_A}s + \omega_n^2},$$

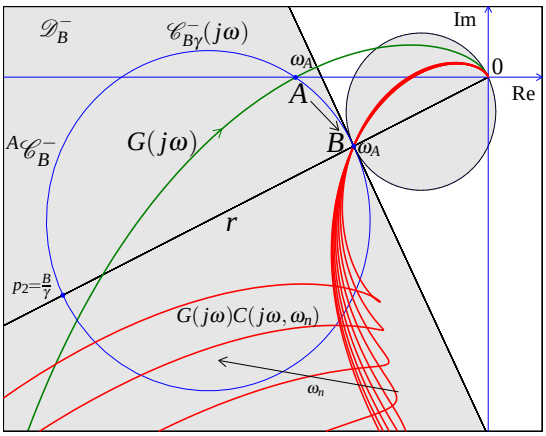

Figure 6. Design of the lead-lag compensators $C(j\omega,\omega_n)$ moving point A to point B.

where $X = X(\omega_A)$ and $Y = Y(\omega_A)$. The frequency response of $C(s,\omega_n)$ at frequency ω_A is equal to the constant value

$$C(j\omega_A,\omega_n) = C(j\omega_A) = \frac{1+jX}{1+jY}. \tag{20}$$

From (12) and (13) it is evident that $A = G(j\omega_A) = M_A e^{j\varphi_A}$ can be moved to $B = M_B e^{j\varphi_B}$ if and only if

$$C(j\omega_A) = M e^{j\varphi} = \frac{M_B}{M_A} e^{j(\varphi_B-\varphi_A)}. \tag{21}$$

From (20) and (21) we obtain the complex equation

$$(M\cos\varphi + jM\sin\varphi)(1+jY) = 1+jX,$$

which is equivalent to the following linear system

$$\begin{bmatrix} 1 & -M\cos\varphi \\ 0 & M\sin\varphi \end{bmatrix} \begin{bmatrix} X \\ Y \end{bmatrix} = \begin{bmatrix} M\sin\varphi \\ M\cos\varphi - 1 \end{bmatrix}.$$

Solving for X and Y, one directly obtains (17)

$$X = \frac{\begin{vmatrix} M\sin\varphi & -M\cos\varphi \\ M\cos\varphi - 1 & M_0\sin\varphi \end{vmatrix}}{M\sin\varphi} = \frac{M-\cos\varphi}{\sin\varphi},$$
$$Y = \frac{\begin{vmatrix} 1 & M\sin\varphi \\ 0 & M\cos\varphi - 1 \end{vmatrix}}{M\sin\varphi} = \frac{\cos\varphi - \dfrac{1}{M}}{\sin\varphi}.$$

The assumption that A belongs to the controllable domain $\mathscr{D}_B^-$ ensures that there exist admissible lead-lag controllers $C(s,\omega_n)$ moving point A to point B which are characterized by positive parameters γ, δ and ω_n, see Definition 4.1. All the admissible values of ω_n are those that satisfy $\delta > 0$ in (19). ■

From (19) and (17) it follows that the gain γ of $C(s,\omega_n)$ at $\omega = \omega_n$ is

$$\gamma = \frac{X}{Y} = \frac{M-\cos\varphi}{\cos\varphi - \frac{1}{M}}. \tag{22}$$

Table 1. Design Problems and design specifications addressed in the paper.

Design Problem	*Phase margin* ϕ_m	*Gain margin* G_m	*Gain crossover frequency* ω_p	*Phase crossover frequency* ω_g
A	×		×	
B		×		×
C	×	×	×	
D	×	×		×
E	×	×		

Note that γ does not depend on ω_A and ω_n, but only on the position of A and B.

Property 4.6 Given two points A and B such that $A \in \mathscr{D}_B^-$, the gain γ in (19) can be graphically determined as shown in Fig. 6:

1) draw the unique circle ${}^A\mathscr{C}_B^-$ that passes through points A and B having its diameter on the straight line r which passes through points 0 and B;
2) the circle ${}^A\mathscr{C}_B^-$ intersects the straight line r at points $p_1 = B$ and $p_2 = B/\gamma$;
3) the gain γ is equal to the modulus of point B over the modulus of point p_2: $\gamma = |B|/|p_2|$.

Proof: It follows directly from Property 4.3 because the circle ${}^A\mathscr{C}_B^-$ on the Nyquist plane coincides with the frequency response $\mathscr{C}_{B\gamma}^-(j\omega)$ of $\mathscr{C}_{B\gamma}^-(s) \in \mathscr{C}_B^-(\gamma)$ and because the intersections of these functions with the straight line r occur at points B and $p_2 = B/\gamma$. ■

5 Synthesis of lead-lag compensators

In this section and in Sec. 6 we will address five different Design Problems, concerning the synthesis of lead-lag compensators $C(s)$ based on the following design specifications, see Tab. 1: ***A)*** phase margin ϕ_m and gain crossover frequency ω_p; ***B)*** gain margin G_m and phase crossover frequency ω_g; ***C)*** phase margin ϕ_m, gain margin G_m and gain crossover frequency ω_p; ***D)*** phase margin ϕ_m, gain margin G_m and phase crossover frequency ω_g; ***E)*** phase margin ϕ_m and gain margin G_m.

Design Problem A: (ϕ_m, ω_p). Given the control scheme of Fig. 4, the transfer function $G(s)$ and the design specifications on the phase margin ϕ_m and on the gain crossover frequency ω_p, design the lead-lag compensator $C(s)$ such that the loop gain transfer function $C(j\omega)G(j\omega)$ passes through point $B_p = e^{j(\pi+\phi_m)}$ for $\omega = \omega_p$.

Solution A: *Let $A_p = G(j\omega_p)$ denote the value of $G(j\omega)$ at the desired gain crossover frequency $\omega = \omega_p$ and let $B_p = e^{j(\pi+\phi_m)}$ denote the point corresponding to the desired phase margin ϕ_m. The set $C_p(s,\omega_n)$ of all the compensators $C(s)$ which solve Design Problem A is obtained from (1) using the parameters*

$$\gamma = \frac{X_p}{Y_p} > 0, \qquad \delta = Y_p \frac{\omega_n^2 - \omega_p^2}{2\omega_n\omega_p} > 0 \tag{23}$$

for all $\omega_n > 0$ such that $\delta > 0$ and with $X_p = X(A_p, B_p)$ and $Y_p = Y(A_p, B_p)$ obtained using (17).

Proof: The design specifications on the phase margin ϕ_m and gain crossover frequency ω_p can be satisfied if and only if the loop gain frequency response $C(j\omega)G(j\omega)$ at $\omega = \omega_p$ is equal to B_p, that is if and only if $B_p = C(j\omega_p)\cdot A_p$. According to Definition 4.1, Design Problem A has a solution only if point A_p belongs to the controllable domain $\mathscr{D}_{B_p}^-$, see the grey region in Fig. 7. The parameters (23) of all the compensators $C_p(s,\omega_n)$ which move point A_p to point B_p are obtained from Property 4.5 when $\omega_A = \omega_p$, $A = A_p$ and $B = B_p$. ■

Examples of the loop gain frequency response $H_p(j\omega,\omega_n) = C_p(j\omega,\omega_n)G(j\omega)$ obtained from (23) for different values of ω_n are plotted in red in Fig. 7 and 8. The blue circle $\mathscr{C}_{B_p\gamma}^-(j\omega)$ represents the frequency

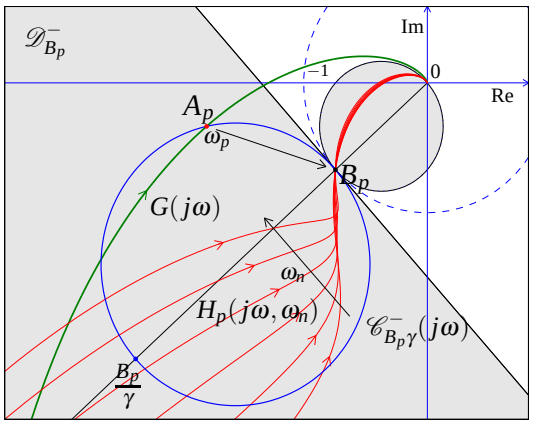

Figure 7. Graphical solution of Design Problem A on the Nyquist plane.

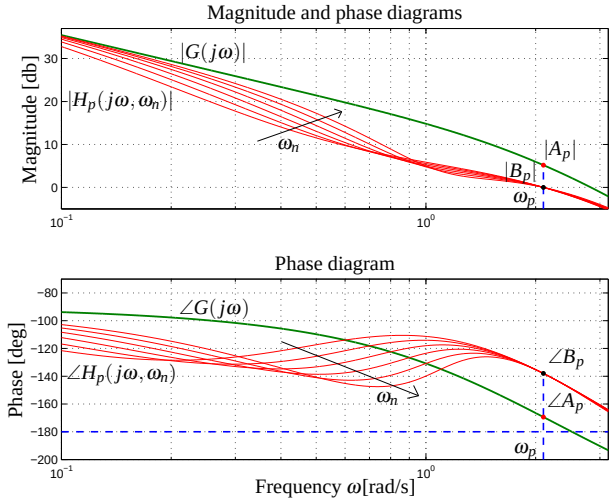

Figure 8. Graphical representation of the solution of Design Problem A on the Bode diagrams.

response of all the functions $\mathscr{C}^-_{B_p\gamma}(s) \in \mathscr{C}^-_{B_p}(\gamma)$ with $\gamma = X_p/Y_p$ given in (23). The free parameter ω_n of $C_p(s,\omega_n)$ can be used to satisfy an additional constraint such as, for example, a desired gain margin G_m as shown in Design Problem C.

Design Problem B: (G_m, ω_g). Given the control scheme of Fig. 4, the transfer function $G(s)$ and design specifications on the gain margin G_m and phase crossover frequency ω_g, design the lead-lag compensator $C(s)$ such that $C(j\omega)G(j\omega)$ passes through point $B_g = -1/G_m$ for $\omega = \omega_g$.

Solution B: *Let $A_g = G(j\omega_g)$ denote the value of $G(j\omega)$ at the desired phase crossover frequency $\omega = \omega_g$ and let $B_g = -1/G_m = M_{B_g} e^{j\varphi_{B_g}}$ denote the point corresponding to the desired gain margin G_m. The set $C_g(s,\omega_n)$ of all the compensators $C(s)$ which solve the Design Problem B is obtained from (1) using*

$$\gamma = \frac{X_g}{Y_g} > 0, \qquad \delta = Y_g \frac{\omega_n^2 - \omega_g^2}{2\omega_n\omega_g} > 0, \tag{24}$$

for all $\omega_n > 0$ such that $\delta > 0$ and with $X_g = X(A_g, B_g)$ and $Y_g = Y(A_g, B_g)$ obtained using (17).

Proof: The design specifications on the gain margin G_m and phase crossover frequency ω_g are satisfied if and only if $B_g = C(j\omega_g)\cdot A_g$. According to Definition 3.1, Design Problem B has a solution only if A_g belongs to $\mathscr{D}^-_{B_g}$, see the grey region in Fig. 9. The parameters (24) of all the compensators $C_g(s,\omega_n)$ which move A_g to B_g are obtained from Property 4.5 when $\omega_A = \omega_g$, $A = A_g$ and $B = B_g$. ■

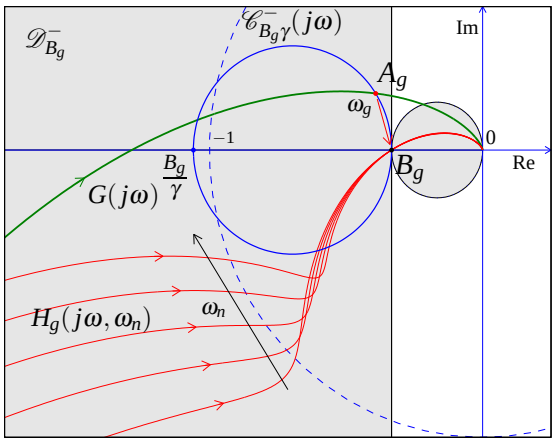

Figure 9. Graphical solution of Design Problem B on the Nyquist plane.

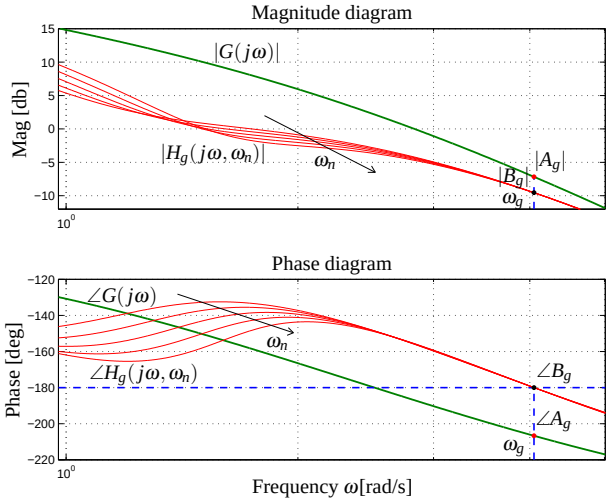

Figure 10. Graphical representation of the solution of Design Problem B on the Bode diagrams.

The loop gain frequency responses $H_g(j\omega,\omega_n) = C_g(j\omega,\omega_n)G(j\omega)$ obtained from (24) for different values of ω_n are plotted in red in Fig. 9 and 10. The blue circle $\mathscr{C}^-_{B_g\gamma}(j\omega)$ in Fig. 9 represents the frequency response of all the functions $\mathscr{C}^-_{B_g\gamma}(s) \in \mathscr{C}^-_{B_g}(\gamma)$ with $\gamma = X_g/Y_g$ given in (24). The free parameter ω_n of $C_g(s,\omega_n)$ can be used to satisfy, for example, a constraint on ϕ_m.

Design Problem C: (ϕ_m , G_m , ω_p). Given the control scheme of Fig. 4, the transfer function $G(s)$ and design specifications on the phase margin ϕ_m, gain margin G_m and gain crossover frequency ω_p, design a lead-lag compensator $C(s)$ such that $C(j\omega)G(j\omega)$ passes through $B_p = e^{j(\pi+\phi_m)}$ for $\omega = \omega_p$ and $B_g = -1/G_m$.

Solution C: *Let $A_p = G(j\omega_p)$ denote the value of $G(j\omega)$ at the desired gain crossover frequency $\omega = \omega_p$, and let $B_p = e^{j(\pi+\phi_m)}$ and $B_g = -1/G_m = M_{B_g} e^{j\varphi_{B_g}}$ denote the complex points corresponding to the desired phase margin ϕ_m and gain margin G_m, respectively. The set $C_p(s,\omega_g)$ of all the lead-lag compensators $C(s)$ which solve Design Problem C is obtained from (1) using*

$$\gamma = \frac{X_p}{Y_p} > 0, \qquad \delta = Y_p \frac{\omega_n^2 - \omega_p^2}{2\omega_n\omega_p} > 0, \tag{25}$$

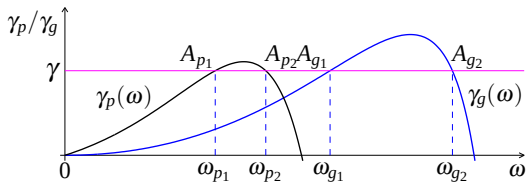

Figure 11. Functions $\gamma_g(\omega)$ (blue line) and $\gamma_p(\omega)$ (black line).

$$\omega_n = \sqrt{\frac{Y_g\,\omega_g - Y_p\,\omega_p}{\frac{Y_g}{\omega_g} - \frac{Y_p}{\omega_p}}} > 0, \tag{26}$$

where the coefficients $X_p = X(A_p, B_p)$, $Y_p = Y(A_p, B_p)$, $X_g = X(A_g, B_g)$ and $Y_g = Y(A_g, B_g)$ are obtained using the inversion formulae (17) with $A_g = G(j\omega_g) = M_{A_g}(\omega_g)\,e^{j\varphi_{A_g}(\omega_g)}$, for all the frequencies ω_g satisfying

$$\gamma = \gamma_g(\omega_g), \tag{27}$$

where $\gamma_g(\omega_g) = X_g/Y_g$ is defined as

$$\gamma_g(\omega_g) = \frac{\frac{M_{B_g}}{M_{A_g}(\omega_g)} - \cos(\varphi_{B_g} - \varphi_{A_g}(\omega_g))}{\cos(\varphi_{B_g} - \varphi_{A_g}(\omega_g)) - \frac{M_{A_g}(\omega_g)}{M_{B_g}}}. \tag{28}$$

A solution $C_p(s, \omega_g)$ of Design Problem C exists only if: 1) the set S_{ω_g} of all the ω_g satisfying (27) is not empty; 2) $A_p \in \mathscr{D}^-_{B_p}$ and $A_g \in \mathscr{D}^-_{B_g}$; 3) ω_n and δ in (25) and (26) are real and positive.

Proof: The design specifications completely define the position of points B_p, A_p and B_g. According to Solution A, the lead-lag compensators $C_p(s, \omega_n)$ which move point $A_p \in \mathscr{D}^-_{B_p}$ to point B_p are obtained using the parameters γ and δ in (25). The free parameter ω_n can now be used to force the loop gain frequency response $C_p(j\omega, \omega_n)G(j\omega)$ to pass through point B_g. This condition can be satisfied only if a frequency ω_g exists such that $C_p(s, \omega_n)$ moves point $A_g = G(j\omega_g) \in \mathscr{D}^-_{B_g}$ to point B_g, that is only if

$$\gamma = \frac{X_g}{Y_g} = \frac{X(A_g, B_g)}{Y(A_g, B_g)}. \tag{29}$$

This relation does not depend on ω_n, but only on the design specifications ϕ_m, G_m and ω_p. Substitution of (17) and (18) into (29) yields (27)-(28). The frequencies $\omega_g \in S_{\omega_g}$ satisfying (27) are acceptable only if the compensator $C_g(s, \omega_n)$ obtained using Solution B is equal to $C_p(s, \omega_n)$. This condition is satisfied only if the two compensators share the same δ, that is only if

$$\delta = Y_p \frac{\omega_n^2 - \omega_p^2}{2\omega_n\omega_p} = Y_g \frac{\omega_n^2 - \omega_g^2}{2\omega_n\omega_g} > 0. \tag{30}$$

Solving (30) with respect to ω_n leads to (26). ■

The solution of (27) can also be obtained graphically by plotting $\gamma_g(\omega)$ and by finding all the frequencies $\omega_g \in S_{\omega_g}$ for which $\gamma_g(\omega_g)$ intersects the horizontal line γ, see Fig. 11. In the example of Fig. 11 it is $S_{\omega_g} = \{\omega_{g1},\ \omega_{g2}\}$ and therefore there are two solutions: $C_p(s, \omega_{g1})$ and $C_p(s, \omega_{g2})$. The corresponding loop gain frequency responses $H_{21}(j\omega) = C_p(j\omega, \omega_{g1})G(j\omega)$ (thin blue line) and $H_{22}(j\omega) = C_p(j\omega, \omega_{g2})G(j\omega)$ (red line) on the Nyquist and the Bode diagrams are shown in Fig. 12 and 13. Both solutions satisfy the design specifications and are acceptable because $\delta > 0$ and $\omega_n > 0$.

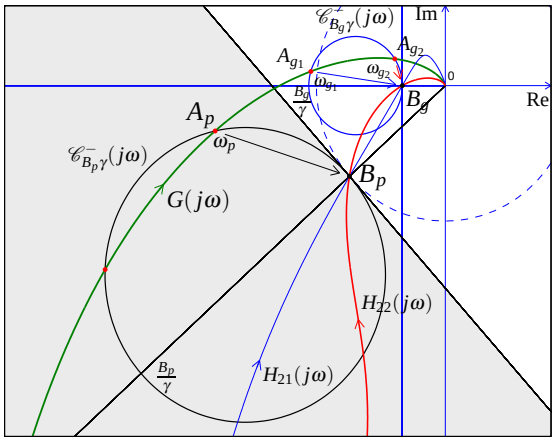

Figure 12. Graphical solution of Design Problem C on the Nyquist plane.

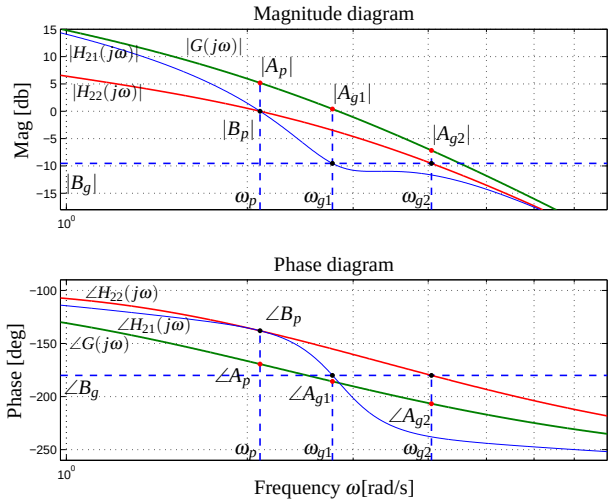

Figure 13. Graphical representation of the solution of Design Problem C on the Bode diagrams.

Property 5.1 The frequencies $\omega_g \in S_{\omega_g}$ satisfying (27) can be graphically determined on the Nyquist plane as shown in Fig. 12:

1) draw the circle $\mathscr{C}^-_{B_p\gamma}(j\omega)$ on the Nyquist plane passing through points A_p and B_p with its diameter on the segment $(B_p, \frac{B_p}{\gamma})$;
2) determine the gain γ of the lead-lag compensators $C_p(s,\omega_g)$ as described in Property 4.6 when $A = A_p$ and $B = B_p$;
3) draw the circle $\mathscr{C}^-_{B_g\gamma}(j\omega)$ having its diameter on the segment $(B_g, \frac{B_g}{\gamma})$;
4) the intersections A_{gi} of $\mathscr{C}^-_{B_g\gamma}(j\omega)$ with $G(j\omega)$ correspond to the frequencies ω_{gi} belonging to the set S_{ω_g}.

Proof: The circles $\mathscr{C}^-_{B_p\gamma}(j\omega)$ (black line) and $\mathscr{C}^-_{B_g\gamma}(j\omega)$ (blue line) shown in Fig. 12 represent, respectively, the frequency responses of $\mathscr{C}^-_{B_p\gamma}(s) \in \mathscr{C}^-_{B_p}(\gamma)$ and $\mathscr{C}^-_{B_g\gamma}(s) \in \mathscr{C}^-_{B_g}(\gamma)$ with $\gamma = X_p/Y_p = X_g/Y_g$ given in (27) and (29). These two circles can be easily determined on the Nyquist plane because A_p, B_p and B_g are known (they follow from the design specifications) and γ is given by the graphical construction described in Property 4.6. A frequency ω_g satisfying (27) exists only if

$$G(j\omega_g)C_\gamma(j\omega_g) = B_g, \tag{31}$$

where $C_\gamma(s)$ is the lead-lag compensator (1) with the value of γ determined as described above. Relation

(31) can be rewritten as

$$G(j\omega) = \frac{B_g}{C_\gamma(j\omega)} = \mathscr{C}^-_{B_g\gamma}(j\omega), \tag{32}$$

with $\omega = \omega_g$, and therefore it can be solved graphically on the Nyquist plane by finding the intersections ω_g of $G(j\omega)$ with $\mathscr{C}^-_{B_g\gamma}(j\omega)$. ■

Design Problem D: (ϕ_m , G_m , ω_g). Given the control scheme of Fig. 4, the transfer function $G(s)$ and the design specifications on the phase margin ϕ_m, gain margin G_m and phase crossover frequency ω_g, design a lead-lag compensator $C(s)$ such that $C(j\omega)G(j\omega)$ passes through point $B_g = -1/G_m$ for $\omega = \omega_g$ and passes through point $B_p = e^{j(\pi+\phi_m)}$.

Solution D: *The given design specifications completely define the points* $A_g = G(j\omega_g)$, $B_p = e^{j(\pi+\phi_m)}$ *and* $B_g = -1/G_m = M_{B_g} e^{j\varphi_{B_g}}$. *The set* $C_g(s,\omega_p)$ *of all the lead-lag compensators* $C(s)$ *which solve Design Problem D is obtained from (1) using*

$$\gamma = \frac{X_g}{Y_g} > 0, \qquad \delta = Y_g \frac{\omega_n^2 - \omega_g^2}{2\omega_n\omega_g} > 0, \tag{33}$$

$$\omega_n = \sqrt{\frac{Y_g\,\omega_g - Y_p\,\omega_p}{\frac{Y_g}{\omega_g} - \frac{Y_p}{\omega_p}}} > 0, \tag{34}$$

where $X_g = X(A_g, B_g)$, $Y_g = Y(A_g, B_g)$, $X_p = X(A_p, B_p)$ *and* $Y_p = Y(A_p, B_p)$ *are obtained using (17) with* $A_p = G(j\omega_p) = M_{A_p}(\omega_p)\, e^{j\varphi_{A_p}(\omega_p)}$, *for all the frequencies* ω_p *satisfying*

$$\gamma = \gamma_p(\omega_p), \tag{35}$$

where $\gamma_p(\omega_p) = X_p/Y_p$ *is defined as*

$$\gamma_p(\omega_p) = \frac{\frac{M_{B_p}}{M_{A_p}(\omega_p)} - \cos(\varphi_{B_p} - \varphi_{A_p}(\omega_p))}{\cos(\varphi_{B_p} - \varphi_{A_p}(\omega_p)) - \frac{M_{A_p}(\omega_p)}{M_{B_p}}}. \tag{36}$$

A solution $C_g(s,\omega_p)$ *of Design Problem D exists only if: 1) the set* S_{ω_p} *of all the* ω_p *satisfying* $\gamma = \gamma_p(\omega_p)$ *is not empty; 2)* $A_g \in \mathscr{D}^-_{B_g}$ *and* $A_p \in \mathscr{D}^-_{B_p}$; *3)* ω_n *and* δ *in (34) are real and positive.*

Proof: The proof is similar to that of Solution C. The positions of $B_p = e^{j(\pi+\phi_m)}$, $B_g = -1/G_m$ and $A_g = G(j\omega_g)$ are directly determined by the given design specifications. The parameters γ and δ in (33) define the structure of the lead-lag compensators $C_g(s,\omega_n)$ which move $A_g \in \mathscr{D}^-_{B_g}$ to B_g. The loop gain $C_g(j\omega,\omega_n)G(j\omega)$ passes through B_p only if a frequency ω_p exists such that $C_g(s,\omega_n)$ moves $A_p = G(j\omega_p) \in \mathscr{D}^-_{B_p}$ to B_p, that is only if the relation $\gamma = \frac{X_p}{Y_p} = \gamma_p(\omega_p)$ given in (35) holds. The frequencies $\omega_p \in S_{\omega_p}$ satisfying (35) are acceptable only if (30) holds. From this relation one directly obtains (34). ■

The graphical solution of (35) can be obtained, see Fig. 11, by plotting $\gamma_p(\omega)$ (the black line) and by finding all the frequencies $\omega_p \in S_{\omega_p}$ where $\gamma_p(\omega_p)$ intersects the horizontal line γ. In Fig. 11 it is $S_{\omega_p} = \{\omega_{p1},\ \omega_{p2}\}$. The corresponding loop gain frequency responses $H_{11}(j\omega) = C_p(j\omega,\omega_{p1})G(j\omega)$ and $H_{21}(j\omega) = C_p(j\omega,\omega_{p2})G(j\omega)$ on the Nyquist and Bode diagrams are the thin blue lines shown in Fig. 14 and 15. These solutions are acceptable only if $\delta > 0$ and $\omega_n > 0$ in (33) and (34).

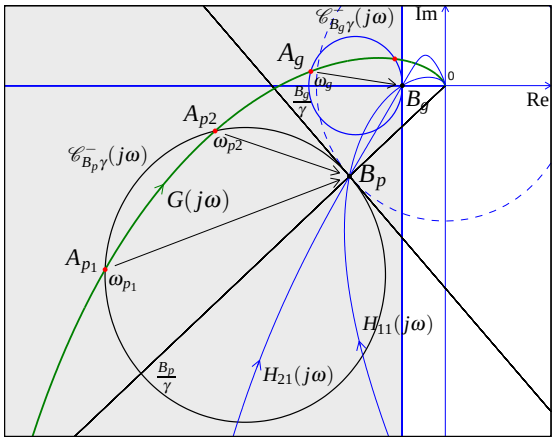

Figure 14. Graphical solution of Design Problem D on the Nyquist plane.

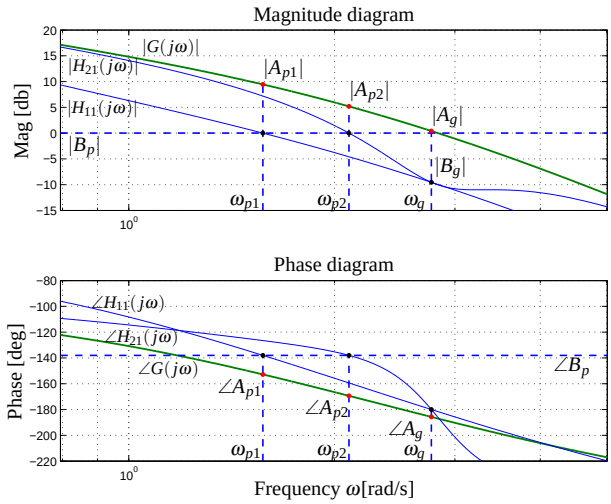

Figure 15. Graphical representation of the solution of Design Problem D on the Bode diagrams.

Property 5.2 The frequencies $\omega_p \in S_{\omega_p}$ satisfying (35) can be graphically determined on the Nyquist plane as follows, see Fig. 14:

1) draw the circle $\mathscr{C}^-_{B_g\gamma}(j\omega)$ on the Nyquist plane passing through points A_g and B_g with its diameter on the segment $(B_g,\ \frac{B_g}{\gamma})$;
2) determine γ as described in Property 4.6 when $A = A_g$ and $B = B_g$;
3) draw the circle $\mathscr{C}^-_{B_p\gamma}(j\omega)$ having its diameter on the segment $(B_p,\ \frac{B_p}{\gamma})$;
4) the points A_{pi} where circle $\mathscr{C}^-_{B_p\gamma}(j\omega)$ intersects $G(j\omega)$ correspond to the frequencies $\omega_{pi} \in S_{\omega_p}$.

This graphical construction holds because a frequency ω_p satisfies (35) only if

$$G(j\omega_p)C_\gamma(j\omega_p) = B_p. \tag{37}$$

This relation can be rewritten as

$$G(j\omega) = \frac{B_p}{C_\gamma(j\omega)} = \mathscr{C}^-_{B_p\gamma}(j\omega), \tag{38}$$

with $\omega = \omega_p$, and can be solved graphically on the Nyquist plane by finding the intersections ω_p of $G(j\omega)$ with $\mathscr{C}^-_{B_p\gamma}(j\omega)$.

6 Design Problem (ϕ_m , G_m) and Graphical Representations.

Let us now consider the following Design Problem E which is a relaxed version of Design Problem C and Design Problem D.

Design Problem E: (ϕ_m , G_m , γ). Given the control scheme of Fig. 4, the transfer function $G(s)$ and the design specifications on the phase margin ϕ_m and gain margin G_m, design a lead-lag compensator $C(s)$ such that the loop gain transfer function $C(j\omega)G(j\omega)$ passes through points $B_p = e^{j(\pi+\phi_m)}$ and $B_g = -1/G_m$ for a value of γ chosen arbitrarily.

Solution E: *Let $B_p = e^{j(\pi+\phi_m)}$ and $B_g = -1/G_m = M_{B_g} e^{j\varphi_{B_g}}$ denote the points corresponding to the desired phase margin ϕ_m and gain margin G_m. The set $C_\gamma(s,\omega_p,\omega_g)$ of all the compensators $C(s)$ which solve Design Problem E is obtained as follows:*

a) *find all the pairs $(\omega_p,\ \omega_g) \in S_{\gamma\omega}$ of frequencies which solve*

$$\gamma = \gamma_p(\omega_p) = \gamma_g(\omega_g), \tag{39}$$

where $\gamma > 0$ is chosen arbitrarily, $S_{\gamma\omega}$ is the set of all the pairs $(\omega_p,\ \omega_g)$ satisfying (39), and $\gamma_p(\omega_p)$ and $\gamma_g(\omega_g)$ are defined in (36) and (28) with $A_p = G(j\omega_p) = M_{A_p}(\omega_p)\, e^{j\varphi_{A_p}(\omega_p)}$ and $A_g = G(j\omega_g) = M_{A_g}(\omega_g)\, e^{j\varphi_{A_g}(\omega_g)}$, respectively.

b) *for each pair $(\omega_p,\ \omega_g) \in S_{\gamma\omega}$ compute*

$$\omega_n = \sqrt{\frac{X_g\,\omega_g - X_p\,\omega_p}{\frac{X_g}{\omega_g} - \frac{X_p}{\omega_p}}} = \sqrt{\frac{Y_g\,\omega_g - Y_p\,\omega_p}{\frac{Y_g}{\omega_g} - \frac{Y_p}{\omega_p}}} > 0, \tag{40}$$

and

$$\delta = Y_p \frac{\omega_n^2 - \omega_p^2}{2\omega_n\omega_p} = Y_g \frac{\omega_n^2 - \omega_g^2}{2\omega_n\omega_g} > 0, \tag{41}$$

where the coefficients $X_p = X(A_p(\omega_p), B_p)$, $Y_p = Y(A_p(\omega_p), B_p)$, $X_g = X(A_g(\omega_g), B_g)$ and $Y_g = Y(A_g(\omega_g), B_g)$ are obtained using the inversion formulae (17).

A solution $C_\gamma(s,\omega_p,\omega_g)$ of Design Problem E exists only if: 1) γ satisfies

$$0 < \gamma < \min\left[\max(\gamma_p(\omega_p)), \max(\gamma_g(\omega_g))\right] \tag{42}$$

2) $S_{\gamma\omega}$ is not empty; 3) points $A_p(\omega_p)$ and $A_g(\omega_g)$ belong, respectively, to the controllable domains $\mathscr{D}^-_{B_p}$ and $\mathscr{D}^-_{B_g}$; 4) parameters ω_n in (40) and δ in (41) are real and positive.

Proof: The design specifications on the phase margin ϕ_m and gain margin G_m completely define the position of points B_p and B_g on the complex plane. A solution $C_\gamma(s,\omega_p,\omega_g)$ exists only if the frequencies ω_p and ω_g satisfy (31) and (37), that is only if they satisfy (39) where $\gamma_p(\omega_p) = X_p/Y_p$ and $\gamma_g(\omega_g) = X_g/Y_g$. For each value of γ satisfying (42), one can find the set $S_{\gamma\omega}$ of all the solutions (ω_p,ω_g) of (39). This relation does not depend on δ and ω_n, but only on the frequencies (ω_p,ω_g) and points (B_p, B_g). Each solution $(\omega_p,\omega_g) \in S_{\gamma\omega}$ corresponds to an acceptable regulator $C_\gamma(s,\omega_p,\omega_g)$ only if ω_n and δ given in (40) and (41) are real and positive. The expressions of ω_n and δ in (40) and (41) are obtained as described in the Solution of Design Problem C by taking into account (39), $X_p = \gamma Y_p$ and $X_g = \gamma Y_g$. ■

The numerical solution of (39) can be obtained graphically by plotting $\gamma_p(\omega)$ and $\gamma_g(\omega)$ and by finding, for each admissible value of γ, all the pairs $(\omega_p,\omega_g) \in S_{\omega_p}$ where $\gamma_p(\omega_p)$ and $\gamma_g(\omega_g)$ intersect the horizontal line γ, see Fig. 11. In the example of Fig. 11 there are four different solutions: $S_{\gamma\omega} = \{(\omega_{p1},\omega_{g1}), (\omega_{p1},\omega_{g2}), (\omega_{p2},\omega_{g1}), (\omega_{p2},\omega_{g2})\}$. The loop gain frequency responses $H_{11}(s)$, $H_{12}(s)$,

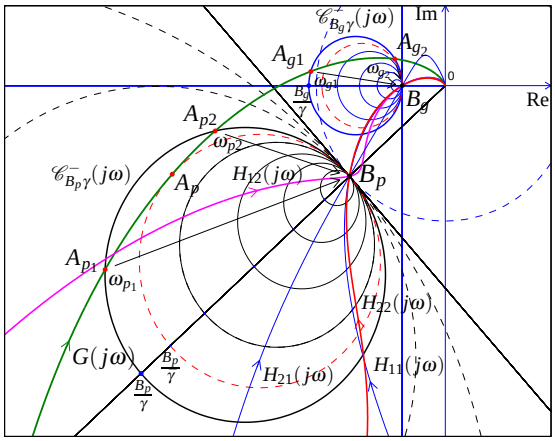

Figure 16. Graphical solution of Design Problem E on the Nyquist plane.

$H_{21}(s)$ and $H_{22}(s)$ of these four solutions on the Nyquist plane are shown in Fig. 16. These solutions are acceptable only if $\delta > 0$ and $\omega_n > 0$ given in (40) and (41) are satisfied.

6.1 *Graphical representations on Nyquist and Nichols planes.*

The solution of the Design Problem E can also be performed graphically on the Nyquist and Nichols planes. Five different graphical representations are now described.

a) $G(j\omega)$**-graphical representation on Nyquist plane**. The frequencies $(\omega_p, \omega_g) \in S_{\omega_p}$ can also be determined on the Nyquist plane using the graphical construction shown in Fig. 16:

1) given points B_p and B_g and a desired value for $\gamma > 0$, draw the circles $\mathscr{C}^-_{B_p\gamma}(j\omega)$ and $\mathscr{C}^-_{B_g\gamma}(j\omega)$ having their diameters on the segments $(B_p,\ B_p/\gamma)$ and $(B_g,\ B_g/\gamma)$;
2) if the frequency response $G(j\omega)$ does not intersect both circles $\mathscr{C}^-_{B_p\gamma}(j\omega)$ and $\mathscr{C}^-_{B_g\gamma}(j\omega)$, the chosen value of γ is not acceptable.
3) otherwise, each pair (ω_p, ω_g) corresponding to the intersections of $G(j\omega)$ with circles $\mathscr{C}^-_{B_p\gamma}(j\omega)$ and $\mathscr{C}^-_{B_g\gamma}(j\omega)$ is a possibile solution for Design Problem E.

This graphical construction hinges on the fact that ω_p and ω_g satisfy relation (39) only if $G(j\omega_p)C_\gamma(j\omega_p) = B_p$ and $G(j\omega_g)C_\gamma(j\omega_g) = B_g$. These relations can be rewritten as

$$\begin{cases} G(j\omega)|_{\omega=\omega_p} = \dfrac{B_p}{C_\gamma(j\omega_p)} = \mathscr{C}^-_{B_p\gamma}(j\omega)\Big|_{\omega=\omega_p} \\ G(j\omega)|_{\omega=\omega_g} = \dfrac{B_g}{C_\gamma(j\omega_g)} = \mathscr{C}^-_{B_g\gamma}(j\omega)\Big|_{\omega=\omega_g} \end{cases} \tag{43}$$

These relations can be solved graphically on the Nyquist plane by finding the frequencies (ω_p, ω_g) where $G(j\omega)$ intersects $\mathscr{C}^-_{B_p\gamma}(j\omega)$ and $\mathscr{C}^-_{B_g\gamma}(j\omega)$.

Using the graphical construction of Fig. 16 it is also easy to determine the maximum value $\bar{\gamma}$ of parameter γ for which a solution of Design Problem E exists: it is the value for which the circle $\mathscr{C}^-_{B_p\bar{\gamma}}(j\omega)$ is tangent to $G(j\omega)$, see the dashed red circles and point A_p in Fig. 16.

b) $G(j\omega)$**-graphical representation on Nichols plane**. The graphical construction described above can be carried out also on the Nichols plane, see Fig. 17. The shapes of $\mathscr{C}^-_{B_p\gamma}(j\omega)$ and $\mathscr{C}^-_{B_g\gamma}(j\omega)$ on the Nichols plane are not circles, but the intersection points A_{p1}, A_{p2}, A_{g1}, A_{g2} with $G(j\omega)$ can still be determined. An advantage of working on the Nichols plane is that $\mathscr{C}^-_{B_p\gamma}(j\omega)$ and $\mathscr{C}^-_{B_g\gamma}(j\omega)$ have the same shape and the same dimension. In fact, these functions differ for just a constant, $\mathscr{C}^-_{B_g\gamma}(j\omega) = (B_g/B_p)\mathscr{C}^-_{B_p\gamma}(j\omega)$, and therefore they differ for just a translation on the Nichols plane.

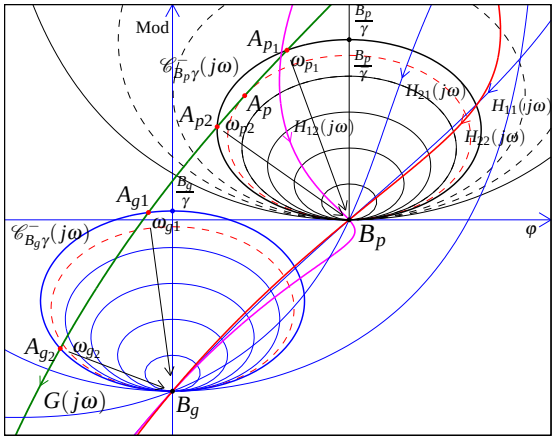

Figure 17. $G(j\omega)$-graphical representation on Nichols plane.

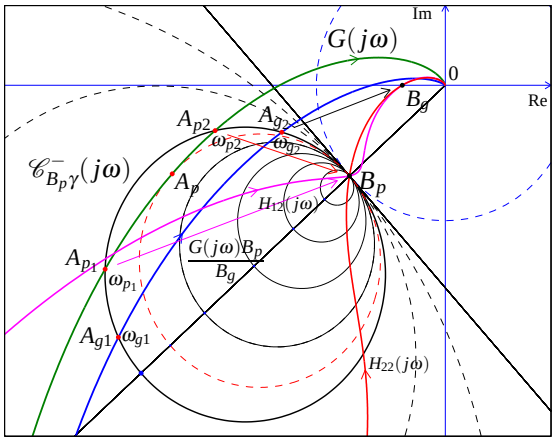

Figure 18. $\mathscr{C}^-_{B_p\gamma}(j\omega)$-graphical representation on Nyquist plane.

c) $\mathscr{C}^-_{B_p\gamma}(j\omega)$**-graphical representation on Nyquist plane**. Multiplying the second equation of system (43) by the constant B_p/B_g one obtains

$$\begin{cases} G(j\omega)\big|_{\omega=\omega_p} = \mathscr{C}^-_{B_p\gamma}(j\omega)\Big|_{\omega=\omega_p} \\ \dfrac{G(j\omega)B_p}{B_g}\Big|_{\omega=\omega_g} = \mathscr{C}^-_{B_p\gamma}(j\omega)\Big|_{\omega=\omega_g} \end{cases} \tag{44}$$

It is evident that these relations can be solved graphically on the Nyquist plane by finding the frequencies (ω_p, ω_g) where $\mathscr{C}^-_{B_p\gamma}(j\omega)$ intersects $G(j\omega)$ and $G(j\omega)B_p/B_g$. A graphical representation of (44) on the Nyquist plane is shown in Fig. 18: the intersections of $\mathscr{C}^-_{B_p\gamma}(j\omega)$ with $G(j\omega)$ provide the frequencies ω_{p1}, ω_{p2}, etc.; the intersections of $\mathscr{C}^-_{B_p\gamma}(j\omega)$ with $G(j\omega)B_p/B_g$ provide the frequencies ω_{g1}, ω_{g2}, etc. The loop gain transfer functions $H_{12}(j\omega)$ and $H_{22}(j\omega)$ corresponding to solutions $(\omega_{p1}, \omega_{g2})$ and $(\omega_{p2}, \omega_{g2})$ are shown in magenta and in red in Fig. 18.

d) $\mathscr{C}_\gamma(j\omega)$**-graphical representation on the Nyquist plane**. Using simple mathematical manipulations,

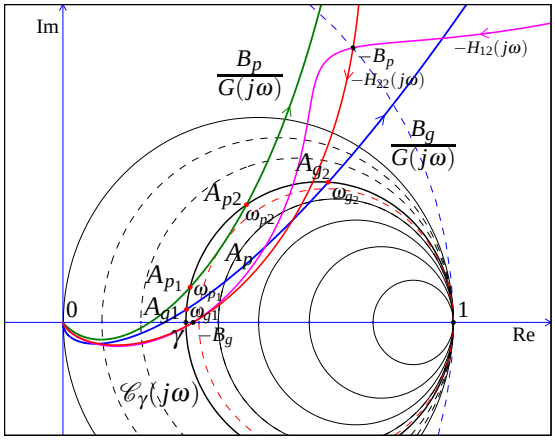

Figure 19. $\mathscr{C}_\gamma(j\omega)$-graphical representation on the Nyquist plane.

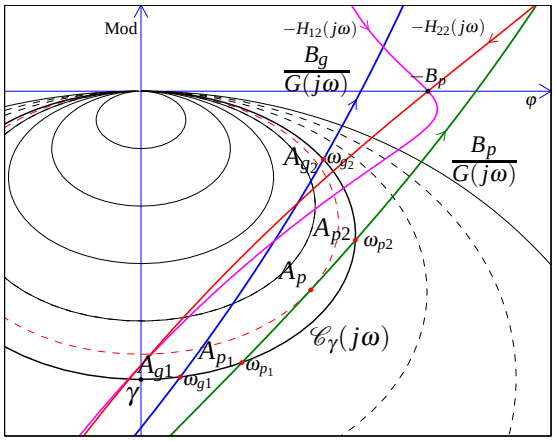

Figure 20. $\mathscr{C}_\gamma(j\omega)$-graphical representation on Nichols plane.

system (43) can be rewritten as

$$\begin{cases} \left.\dfrac{B_p}{G(j\omega)}\right|_{\omega=\omega_p} = \mathscr{C}_\gamma(j\omega)\big|_{\omega=\omega_p} \\ \left.\dfrac{B_g}{G(j\omega)}\right|_{\omega=\omega_p} = \mathscr{C}_\gamma(j\omega)\big|_{\omega=\omega_g} \end{cases} \tag{45}$$

These equations can be solved graphically on the Nyquist plane by finding the frequencies (ω_p, ω_g) where $\mathscr{C}_\gamma(j\omega)$ intersects $B_p/G(j\omega)$ and $B_g/G(j\omega)$. A graphical representation of (45) on the Nyquist plane is shown in Fig. 19. The intersections with $B_p/G(j\omega)$ provide the frequencies ω_{p1}, ω_{p2}, etc. and the intersections with $B_g/G(j\omega)$ provide ω_{g1}, ω_{g2}, etc. Note that in Fig. 19 the points $-B_p$ and $-B_g$, and the two loop gain frequency responses $-H_{12}(s)$ and $-H_{22}(s)$ have also been reported: the relative position of these points and functions with respect to point 1 is the same of points B_p and B_g and $H_{12}(s)$ and $H_{22}(s)$ with respect to -1.

e) $\mathscr{C}_\gamma(j\omega)$-graphical representation on Nichols plane. Equations (45) can be solved graphically on the Nichols plane as well, as shown in Fig. 20. In this case the shapes of $\mathscr{C}_\gamma(j\omega)$ are not circles, but the graphical representation is more precise for small values of the modulus. This graphical representation is similar to the one presented in '(Yeung et al. 1998)' for the solution of Design Problems C and D.

7 Numerical examples

Example 1. All the graphical representations from Fig. 7 to Fig. 20 used in the solutions of Design Problems A, B, C, D and E refer to the system

$$G(s)=\frac{40(s+1)}{s(s+1.5)^2(s+3)}$$

with the following design specifications: phase margin $\phi_m=42^\circ$, gain margin $G_m=3$, gain crossover frequency $\omega_p=2.1$ and phase crossover frequency $\omega_g=4.05$. The modulus and the phase of points $B_p=M_{B_p}e^{j\varphi_{B_p}}=e^{j(\pi+\phi_m)}$ and $B_g=M_{B_g}e^{j\varphi_{B_g}}=-1/G_m$ are $M_{B_p}=1$, $\varphi_{B_p}=222^\circ$, $M_{B_g}=0.333$ and $\varphi_{B_g}=180^\circ$. The value of γ obtained in (23), (24), (27), (33) and used in Design Problem E is

$$\gamma=\frac{X_p}{Y_p}=\frac{Y_g}{X_g}=0.315.$$

The frequencies ω_{p1}, $\omega_{p2}=\omega_p$, $\omega_{g1}=\omega_g$ and ω_{g2} (27), (35) and (39) are $\omega_{p1}=1.57$, $\omega_{p2}=2.1$, $\omega_{g1}=2.77$ and $\omega_{g2}=4.05$. The corresponding points $A_{p1}=G(j\omega_{p1})$, $A_{p2}=A_p=G(j\omega_{p2})$, $A_{g1}=A_g=G(j\omega_{g1})$ and $A_{g2}=G(j\omega_{g2})$ on the frequency response $G(j\omega)$ are

$$A_{p1}=2.97\,e^{-j152.7^\circ},\quad A_{p2}=1.82\,e^{-j169.4^\circ},$$
$$A_{g1}=1.05\,e^{j174.3^\circ},\quad A_{g2}=0.44\,e^{j153.3^\circ}.$$

Let us now consider the solutions of the previously described Design Problems separately.

Design Problems A: (ϕ_m, ω_p). The parameters X_p, Y_p and γ corresponding to A_p and B_p are $X_p=-0.5824$, $Y_p=-1.8491$ and $\gamma=X_p/Y_p=0.315$. The set of regulators $C_p(s,\omega_n)$ satisfying Design Problems A are

$$C_p(s,\omega_n)=\frac{s^2+X_p\frac{\omega_p^2-\omega_n^2}{\omega_p}s+\omega_n^2}{s^2+Y_p\frac{\omega_p^2-\omega_n^2}{\omega_p}s+\omega_n^2},\tag{46}$$

for $0<\omega_n<\omega_p=2.1$. The loop gain transfer function $H_p(j\omega,\omega_n)=C_p(s,\omega_n)G(j\omega)$ for $\omega_n=\{[0.6:0.1:1.1]\}$ is represented by red lines in Fig. 7 and 8.

Design Problems B: (G_m, ω_g). The parameters X_g, Y_g and γ corresponding to A_g and B_g are $X_g=-0.295$, $Y_g=-0.937$ and $\gamma=X_g/Y_g=0.315$. The set of regulators $C_g(s,\omega_n)$ satisfying the Design Problems B are

$$C_g(s,\omega_n)=\frac{s^2+X_g\frac{\omega_g^2-\omega_n^2}{\omega_g}s+\omega_n^2}{s^2+Y_g\frac{\omega_g^2-\omega_n^2}{\omega_g}s+\omega_n^2},\tag{47}$$

for $0<\omega_n<\omega_g=4.05$. The loop gain transfer function $H_g(j\omega,\omega_n)=C_g(s,\omega_n)G(j\omega)$ is represented by red lines in Fig. 9 and 10 for $\omega_n=\{[1.2:0.1:1.6]\}$.

Design Problems C: (ϕ_m, G_m, ω_p). The parameters X_p, Y_p and γ corresponding to A_p and B_p are $X_p=-0.582$, $Y_p=-1.849$ and $\gamma=X_p/Y_p=0.315$. The two solutions of (27) are $S_{\omega_g}=\{\omega_{g1},\omega_{g2}\}=\{2.77,4.05\}$. Substitution into (25) and (26) yields $\delta=-0.571$ and $\omega_n=2.85$ when $\omega=\omega_{g1}$; $\delta=5.14$ and $\omega_n=0.37$ when $\omega=\omega_{g2}$. Only the second solution where $\delta>0$ is acceptable:

$$C_p(s,\omega_{g2})=\frac{s^2+1.186\,s+0.134}{s^2+3.765s+0.134}.\tag{48}$$

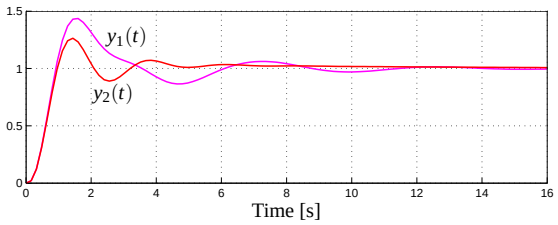

Figure 21. Step responses $y_1(t)$ (magenta line) and $y_2(t)$ (red line) of the closed loop system when, respectively, regulators $C_\gamma(s,\omega_{p1},\omega_{g2})$ in (49) and $C_p(s,\omega_{g2})$ in (48) are used.

The corresponding loop gain transfer function $H_{22}(j\omega)=C_p(s,\omega_{g2})G(j\omega)$ is plotted in red in Fig. 12 and 13.

Design Problems D. (ϕ_m, G_m, ω_g). The parameters which correspond to points A_g and B_g are $X_g=-6.778$, $Y_g=-21.52$ and $\gamma=X_p/Y_p=0.315$. The two solutions of (35) are $S_{\omega_p}=\{\omega_{p1},\omega_{p2}\}=\{1.57,2.1\}$. Substitution into (33) and (34) yields $\delta=-8.82$ and $\omega_n=4.13$ when $\omega=\omega_{p1}$; $\delta=-0.571$ and $\omega_n=2.85$ when $\omega=\omega_{p2}$. Neither solution is acceptable because in both cases $\delta<0$. The loop gain transfer functions $H_{11}(j\omega)$ and $H_{21}(j\omega)$ are the blue lines shown in Fig. 14 and 15.

Design Problems E: (ϕ_m, G_m, γ). Given B_p, B_g and γ, the four solutions $(\omega_{pi},\omega_{gj})$ of equation (39) can be graphically determined as shown in Fig. 11. By substitution into (40) and (41) one obtains only two acceptable and stable regulators $C_\gamma(s,\omega_p,\omega_g)$. The first one is obtained for $(\omega_{p1},\omega_{g2})$, $\delta=1.691$ and $\omega_n=1.338$:

$$C_\gamma(s,\omega_{p1},\omega_{g2})=\frac{s^2+1.065s+1.791}{s^2+3.382s+1.791}. \tag{49}$$

The corresponding loop gain transfer function $H_{12}(j\omega)=C_\gamma(j\omega,\omega_{p1},\omega_{g2})G(j\omega)$ is shown on the Nyquist plane in Fig. 16 and on the Nichols plane in Fig. 17. The second acceptable solution $C_\gamma(s,\omega_{p2},\omega_{g2})$ is obtained for $(\omega_{p2},\omega_{g2})$, $\delta=5.14$ and $\omega_n=0.37$, and it coincides with the $C_p(s,\omega_{g2})$ given in (48). The other two solutions are not acceptable. The step responses $y_1(t)$ and $y_2(t)$ of the closed loop system when, respectively, regulators $C_\gamma(s,\omega_{p1},\omega_{g2})$ in (49) and $C_p(s,\omega_{g2})$ in (48) are used, are shown in Fig. 21.

Example 2. Let us consider the transfer function proposed in '(Yeung et al. 1998)':

$$G(s)=\frac{5000}{s(s+5)(s+10)}, \tag{50}$$

with the following design specifications: phase margin $\phi_m=42^\circ$, gain crossover frequency $\omega_p=9$ rad/s and gain margin $G_m=4$. The synthesis of the lead-lag controllers $C_p(s,\omega_{g2})$ follows the lines described in Design Problem C. The modulus and the phase of $B_p=M_{B_p}e^{j\varphi_{B_p}}=e^{j(\pi+\phi_m)}$, $A_p=M_{A_p}e^{j\varphi_{A_p}}=G(j\omega_p)$ and $B_g=M_{B_g}e^{j\varphi_{B_g}}=-1/G_m$ are $M_{B_p}=1$, $\varphi_{B_p}=222^\circ$, $M_{A_p}=4.01$, $\varphi_{A_p}=167.1^\circ$, $M_{B_g}=0.25$ and $\varphi_{B_g}=180^\circ$. From A_p and B_p one obtains $X_p=-0.397$, $Y_p=-4.198$ and $\gamma=X_p/Y_p=0.0946$. The two solutions of (27) are $S_{\omega_g}=\{\omega_{g1},\omega_{g2}\}=\{11.37,20.71\}$, see Fig. 22. Only the one corresponding to ω_{g2} is acceptable, and gives $\delta=17.68>0$ and $\omega_n=2.28$. The corresponding lead-lag regulator is

$$C_p(s,\omega_{g2})=\frac{s^2+3.347\,s+5.198}{s^2+35.36\,s+5.198}. \tag{51}$$

The graphical constructions corresponding to the synthesis of the lead-lag compensator $C_p(s,\omega_{g2})$ on the Nyquist, Bode and Nichols planes are shown in Fig. 23-Fig. 25. The loop gain transfer function $H_2(j\omega)=C_p(j\omega,\omega_{g2})G(j\omega)$ is the red line shown in the figures.

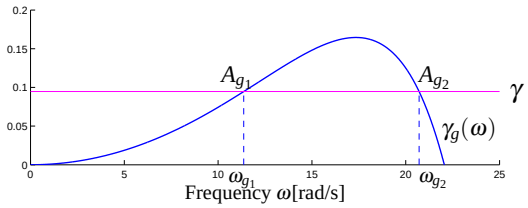

Figure 22. Example 2: function $\gamma_g(\omega)$ intersects the value γ at frequencies $\{\omega_{g1},\ \omega_{g2}\} = \{11.37, 20.71\}$.

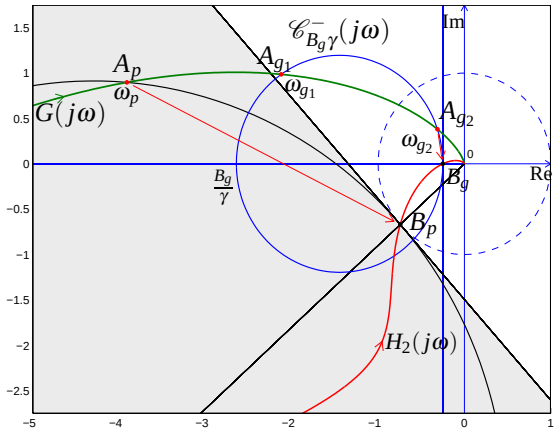

Figure 23. Example 2: synthesis and graphical interpretation of the lead-lag compensators $C_p(s, \omega_{g2})$ on the Nyquist plane.

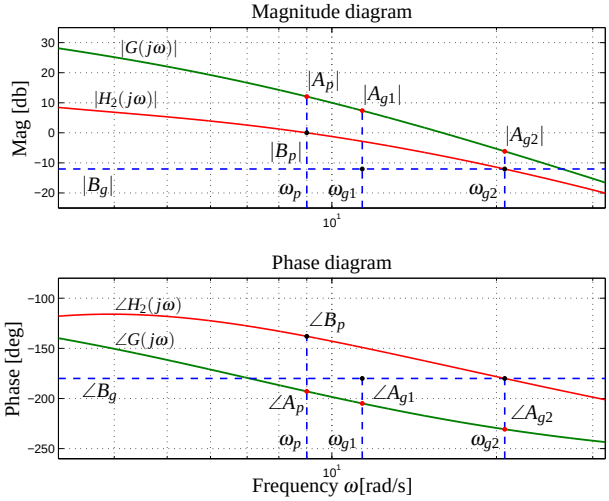

Figure 24. Example 2: graphical representation of the solution on the Bode diagrams.

8 Conclusion

In this paper a general structure for a second order lead-lag compensator has been given and the analytical and graphical solutions of five different Design Problems, given in terms of phase margin, gain margin and phase or gain crossover frequency, have been presented. The analytical solutions of the Design Problems are based on the use of the *inversion formulae* approach, and the graphical solutions have been given both in the Nyquist and Nichols planes.

The design of lead-lag compensators using the analytical and graphical method presented in this paper is simple and suitable both for educational and practical purposes. It has also been shown that the techniques presented here for the design of lead-lag compensators with standard specifications on the stability margins and the crossover frequencies outperform the existing ones.

Future works will include an important extension of the techniques presented in this paper to situations

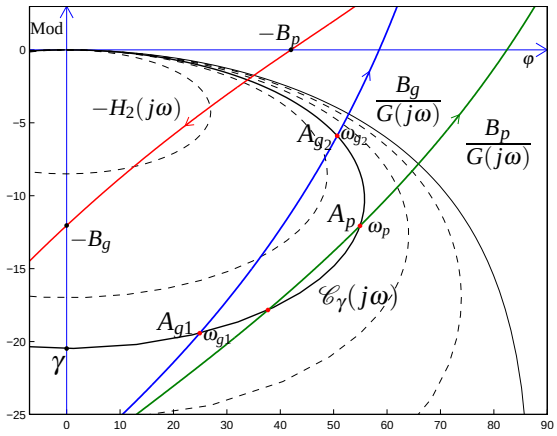

Figure 25. Example 2: Graphical determination on the Nichols plane of the frequencies $(\omega_{g1}, \omega_{g2})$ where $\mathscr{C}_\gamma(j\omega)$ intersects function $B_g/G(j\omega)$.

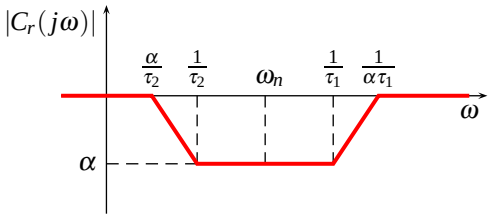

Figure 26. Asymptotic amplitude Bode diagram of compensator $C_r(s)$.

in which only one or two of the specifications considered here are assigned (e.g., the phase margin and the gain crossover frequency), and the remaining degree of freedom is exploited to reduce/minimize additional parameters such as the settling time, the damping ratio or to increase the sensitivity margin. We also aim to adapt the analytical, numerical and graphical techniques presented in this paper to the discrete-time domain.

Appendix A: Lead-lag compensators with real poles and real zeros

The classical form $C_r(s)$ of the lead-lag compensator with real poles is

$$C_r(s) = \frac{(1+\tau_1 s)(1+\tau_2 s)}{(1+\alpha\tau_1 s)(1+\frac{\tau_2}{\alpha}s)} \tag{52}$$

with $0 < \tau_1 < \tau_2$ and $0 < \alpha < 1$. The asymptotic amplitude Bode diagram of $C_r(j\omega)$ is shown in Fig. 26. The relations that link the parameters τ_1, τ_2 and α of compensator $C_r(s)$ to parameters γ, δ and ω_n of compensator $C(s)$ are

$$\tau_1 = \frac{\gamma\delta - \sqrt{\gamma^2\delta^2 - 1}}{\omega_n}, \qquad \tau_2 = \frac{\gamma\delta + \sqrt{\gamma^2\delta^2 - 1}}{\omega_n},$$

$$\alpha = \frac{\delta - \sqrt{\delta^2 - 1}}{\gamma\delta - \sqrt{\gamma^2\delta^2 - 1}}; \qquad \gamma = \frac{\tau_1 + \tau_2}{\alpha\tau_1 + \frac{\tau_2}{\alpha}},$$

$$\omega_n = \frac{1}{\sqrt{\tau_1\tau_2}}, \qquad \delta = \frac{\omega_n}{2}\left(\alpha\tau_1 + \frac{\tau_2}{\alpha}\right).$$

For compensator $C_r(s)$ the controllable domain $\mathscr{D}^-$ coincides with the controllable domain $\mathscr{D}_1^-$ of compensator $C(s)$, see Fig. 3.

References

Åström, K.J., and Hagglund, T. (1984), "Automatic Tuning of Simple Regulators with Specifications on Phase and Amplitude Margins," *Automatica*, vol. 20, no.5, pp. 645–651.

Flores, S.S., Valle, A.M., and Castillejos, B.A. (2007), "Geometric Design of Lead/Lag Compensators Meeting a Hinf Specification," in *4th ICEEE International Conference On Elettrical and Electronics Engineering*, Mexico City, Mexico, 5–7 Sep 2007.

Franklin, G., Powell, J.D., and Emami-Naeini, A. (2006), Feedback Control of Dynamic Systems, Prentice Hall.

Fung, H.W., Wang, Q.G., and Lee T.H. (1998), "PI tuning in terms of gain and phase margins," *Automatica*, vol. 34, no. 9, pp. 1145–1149.

Ho, W.K., Gan, O.P., Tay, E.B., and Ang, E.L. (1996), "Performance and gain and phase margins of well-known PID tuning formulas," *IEEE Transactions on Control Systems Technology*, vol. 4, pp. 473–477.

Lee, C.H. (2004), "A survey of PID controller designed based on gain and phase margins," *International Journal of Computational Cognition*, vol. 2, no. 3, pp. 63–100.

Marro, G., and Zanasi, R. (1998), "New Formulae and Graphics for Compensator Design," in *IEEE International Conference On Control Applications*, Trieste, Italy, 1–4 Sep 1998.

Messner, W.C., Bedillion, M.D., Xia, L., and Karns, D.C. (2007), "Lead and Lag Compensators with Complex Poles and Zeros: design formulas for modeling and loop shaping," *IEEE Control System Magazine*, vol. 27, no. 1, pp. 44–54.

Messner, W. (2009), "Formulas for Asymmetric Lead and Lag Compensators," in *American Control Conference*, Hyatt Regency Riverfront, St. Louis, MO, USA, 10–12 June 2009.

Ntogramatzidis, L., and Ferrante, A. (2011), "Exact Tuning of PID Controllers in Control Feedback Design," *IET Control Theory & Applications*, 5(4): 565–578.

Phillips, C.L. (1985), "Analytical Bode Design of Controllers," *IEEE Transactions on Education*, vol. E-28, no. 1, pp. 43–44.

Wang, Q.G., Fung, H.W., and Zhang, Y. (1999), "PID tuning with exact gain and phase margins," *ISA Transactions*, 38, 243–249.

Yeung, K.S., Wong, K.W., and Chen, K.L. (1998) "A Non-Trial-and-Error Method for Lag-Lead Compensator Design," *IEEE Transactions on Education*, vol. E-41, no. 1, 76–80.

Zanasi, R., and Morselli, R. (2009), "Discrete Inversion Formulas for the Design of Lead and Lag Discrete Compensators," *ECC - European Control Conference*, Budapest, Hungary, 23–26 Aug 2009.